L-608

NATIONAL ADVISORY COMMITTEE FOR AERONAUTICS

WARTIME REPORT

ORIGINALLY ISSUED

April 1945 as
Memorandum Report L5D06

COMPARISON OF PREDICTED AND ACTUAL CONTROL-FIXED STABILITY AND CONTROL CHARACTERISTICS OF A DOUGLAS A-26B AIRPLANE

By Harold L. Crane and Sigurd A. Sjoberg

Langley Memorial Aeronautical Laboratory
Langley Field, Va.

NACA

WASHINGTON

MR No. L5D06

NATIONAL ADVISORY COMMITTEE FOR AERONAUTICS

MEMORANDUM REPORT

for the

Army Air Forces, Air Technical Service Command

COMPARISON OF PREDICTED AND ACTUAL CONTROL-FIXED STABILITY AND CONTROL CHARACTERISTICS OF A DOUGLAS A-26B AIRPLANE

By Harold L. Crane and Sigurd A. Sjoberg

SUMMARY

This report presents a comparison of some of the flying qualities of the A-26B airplane predicted from the physical dimensions of the airplane with the actual flying qualities as determined by Langley flight tests.

No estimate of control forces, of effects of power on stability, or of adverse aileron yaw has been made. There was good agreement between the measured and predicted stick-fixed neutral points, stick-fixed maneuver points, elevator deflections required for trim, aileron effectiveness, and rudder-fixed directional stability. The results indicate that the control-fixed, power-off stability and control characteristics of a conventional airplane can be predicted from the dimensions of the airplane and from general wind-tunnel data now available with sufficient accuracy for design purposes.

INTRODUCTION

At the request of the Army Air Forces, Air Technical Service Command, flight tests have been made to determine the flying qualities of a Douglas A-26B airplane. These tests were reported in references 1 to 3. It has been requested by the Air Technical Service Command that a report comparing predicted and actual flying qualities be prepared in conjunction with flight measurements of the flying qualities of an airplane. In the present report some of the flying qualities of the airplane are

predicted from the physical dimensions of the airplane and compared with the actual flying qualities. Discussion of errors in the predicted flying qualities and the probable sources of error is included. No control-force data are presented because no satisfactory method of estimating the hinge moments is known. Neither the effects of power on stability nor the amount of adverse aileron yaw were predicted because methods of calculation were not sufficiently well developed, but it is hoped to present these calculations at a later date.

THE AIRPLANE

The Douglas A-26B airplane is a three-place, twin-engine, midwing, attack-bombing airplane having double-slotted flaps and a retractable tricycle-type landing gear. All control surfaces were sealed. Figure 1 is a three-view drawing of the airplane. Dimensions used in the calculations are listed below:

Weight (assumed for calculations), lb	29,000
Wing	
Area (including ailerons and fuselage), sq ft	540
Span, ft	70
Aspect ratio	9.08
Taper ratio	0.45
Mean aerodynamic chord, in.	97.53
Location of leading-edge mean aerodynamic chord (in. aft of leading edge of root chord)	6.1
Airfoil section, root	65,2-215 a = 0.8 b = 1.0
tip	65,2-215 a = 0.5 b = 1.0
Incidence, deg, root,	2
tip,	1
Dihedral (top face of front beam), deg	4.5
Sweepback of leading edge, deg	1.9
Wing flaps	
Type	double slotted
Flap span (including nacelle and fuselage cut-outs), percent wing span	65
(excluding nacelle and fuselage cut-outs), percent wing span	44
Area, sq ft	65.9
Chord, (main flap only) percent wing chord	25
Deflection (maximum in flight), deg	50

Ailerons

Type	sealed internal balance
Location, along wing semispan, percent wing semispan	65 to 96.5
Chord (aft of hinge line), percent wing chord	21
Area (aft of hinge line, total of two ailerons including tabs), sq ft	27.2
Deflection (maximum under no load), deg	20 up 15 down
Balance-tab area (total of two), sq ft	2.3
Balance-tab linkage ratio	0.36
Trimming tab area (left aileron), sq ft	1.15
Tab chord, percent wing chord	8.00

Horizontal tail

Total area (including section through fuselage), sq ft	116.1
Span, ft	22.69
Stabilizer area, including elevator balance area forward of hinge line, sq ft	83.4
Elevator area (aft of hinge line), sq ft	32.66
Balance area, forward of hinge line	10.3
Incidence, deg	0
Dihedral, deg	10.58
Trimming tab area, total sq ft	2.6
Tail length (from elevator hinge line to 25 percent mean aerodynamic chord of wing), ft	30.05
Elevator deflection (maximum under no load), deg	29 up 19 down

Vertical tail

Total area (excluding dorsal), sq ft	71.35
Fin area (including rudder balance area forward of hinge line), sq ft	48.23
Rudder area (aft of hinge line), sq ft	23.1
Height above fuselage, ft	10
Rudder deflection (maximum under no load), deg	$19\frac{1}{2}$ right and left

Engines (2)	Pratt & Whitney R-2800-2SBG
Rating	
Take-off	2000 hp - 52 in. Hg - 2700 rpm
Military	1950 hp - 50.5 in. Hg - 2700 rpm - 1500 ft 1600 hp - 47.0 in. Hg - 2700 rpm - 12,000 ft
Max. continuous	1500 hp - 41.5 in. Hg - 2400 rpm - 5300 ft
Propellers (2)	
Type	Hamilton Standard
Diameter, ft	12.5
Number of blades	3
Gear ratio	2:1
Service center-of-gravity range, percent mean aerodynamic chord	18 to 32
Wheels - smooth contour	
Main wheels, in.	diameter 47 - width 17
Nose wheel, in.	diameter 36 - width 13

SYMBOLS

W	airplane weight, pounds
S	wing area, including section through fuselage and the ailerons, square feet
b	wing span, feet
α_T	angle of attack of thrust axis, degrees
C_L	airplane lift coefficient, nW/qS_w
n	normal acceleration, gravitational units
q	free-stream dynamic pressure, pounds per square foot
$dC_L/d\alpha$	variation of lift coefficient with angle of attack
C_m	pitching-moment coefficient of airplane, $C_m = \frac{M}{qSc}$

M	airplane pitching moment, foot-pounds
c	mean aerodynamic chord of wing, feet
dC_m/dC_L	variation of pitching-moment coefficient with lift coefficient
q_t	dynamic pressure at tail, pounds per square foot
l_t	distance parallel to thrust axis from airplane center of gravity to elevator hinge line, feet
k	factor for correction of propeller downwash for effects of wing and fuselage
$d\epsilon/d\alpha$	variation of downwash angle at tail with angle of attack
l_p	distance from center of gravity to propeller plane measured parallel to thrust axis, feet
D	propeller diameter, feet
δ	control-surface deflection measured from neutral position, degrees
ρ	mass density of air, slugs per cubic foot
τ	elevator effectiveness factor, $d\alpha_t/d\delta_e$
C_N	coefficient of force normal to thrust axis
$dC_{N_p}/d\alpha$	rate of change of normal-force coefficient of propeller with angle of attack
$\left(\frac{d\epsilon}{d\alpha}\right)_p$	rate of change of upwash at propeller plane with angle of attack
S_n	projected side area of nacelle, square feet
l_n	length of nacelle, feet
bhp	brake horsepower

η	propeller efficiency
a	spanwise distance from airplane center line to thrust line, feet
V	true airspeed, feet per second
p	rolling velocity, radians per second
C_{l_δ}	variation of rolling-moment coefficient with aileron deflection
C_{l_p}	variation of rolling-moment coefficient with pb/2V
K	aileron effectiveness factor $d\alpha_w/d\delta_a$
pb/2V	helix angle described by wing tip, radians
C_n	yawing-moment coefficient of airplane $C_n = \frac{N}{qSb}$
β	angle of sideslip, degrees
$\left(\frac{dC_Y}{d\psi}\right)_p$	rate of change of side force coefficient of propeller with angle of yaw
$\left(\frac{dC_{N_t}}{d\beta}\right)$	rate of change of normal-force coefficient of vertical tail with angle of sideslip

Subscripts

w	wing
t	tail
f	fuselage
n	nacelle
p	propeller
e	elevator
a	aileron
r	rudder
T	thrust axis

METHOD OF ANALYSIS, RESULTS, AND COMPARISON WITH FLIGHT DATA

I. Longitudinal Stability and Control

A. Stick-fixed neutral point

The neutral stability point of the airplane was determined for the gliding condition (engines idling, flaps up, and landing gear retracted) at high speeds. The first step was to determine the value of dC_m/dC_L, the rate of change of pitching-moment coefficient with lift coefficient, at two center-of-gravity positions for the various airplane components.

A discussion of the methods used in determining the effects of the various components follows:

1. Wing aerodynamic center

The wing aerodynamic center was assumed to be at 25 percent mean aerodynamic chord. Wind-tunnel tests of a 65,3-118, a = 1.0 airfoil reported in reference 4 showed the aerodynamic center of this similar airfoil to be at 25 percent mean aerodynamic chord.

2. Fuselage and nacelle effect

The rate of change of pitching-moment coefficient C_m with lift coefficient C_L for fuselage and nacelles was determined by the method outlined in reference 5.

3. Horizontal-tail effect

The rearward shift in neutral point due to the horizontal tail was calculated from the formula:

$$\left(\frac{dC_m}{dC_L}\right)_t = \frac{\left(\frac{dC_L}{d\alpha}\right)_t}{\left(\frac{dC_L}{d\alpha}\right)_w} \frac{S_t}{S_w} \frac{l_t}{c} \frac{q_t}{q} \left(1 - \frac{d\epsilon}{d\alpha}\right)$$

A value of $\frac{q_t}{q} = 0.9$ was used in the calculations. The slope of the lift curve of the tail $\left(\frac{dC_L}{d\alpha}\right)_t$ was obtained from reference 6 and was found to be 0.066 per degree. From unpublished low-drag airfoil data a value of wing lift-curve slope $\left(\frac{dC_L}{d\alpha}\right)_w = 0.0868$ was obtained for use in the calculations. A value of $d\epsilon/d\alpha$ of 0.41 was obtained from reference 6.

4. Propeller normal-force effect

The propeller normal-force effect was obtained from the formula given in reference 5:

$$\left(\frac{dC_m}{dC_L}\right)_{C_{N_p}} = -\frac{\left[1 + \left(\frac{d\epsilon}{d\alpha}\right)_p\right] l_p \frac{\pi}{4} D^2 \frac{dC_{N_p}}{d\alpha}}{\left(\frac{dC_L}{d\alpha}\right)_w Sc}$$

A value of the upwash factor $\left[1 + \left(\frac{d\epsilon}{d\alpha}\right)_p\right] = 1.25$ was obtained from figure 8, reference 7, and a value of the variation of propeller normal-force coefficient with angle of attack $\frac{dC_{N_p}}{d\alpha} = 0.12$ from figure 6, reference 8.

5. Propeller downwash effect

The effect of propeller downwash on $\left(\frac{dC_m}{dC_L}\right)_t$ was calculated by the formula given in reference 5:

$$\left(\frac{dC_m}{dC_L}\right)_{\epsilon_p} = \frac{\left(\frac{dC_m}{dC_L}\right)_t \left(\frac{dC_{N_p}}{d\alpha}\right) \left[1 + \left(\frac{d\epsilon}{d\alpha}\right)_p\right] k}{2\left(1 - \frac{d\epsilon}{d\alpha}\right)}$$

This formula was derived from consideration of the mass flow through the propeller and the change in

its momentum perpendicular to the relative wind produced by the propeller. The factor k from reference 5, which is equal to approximately 0.5 was included to take into account the effects of the wing, fuselage, and other factors on the propeller downwash. The effect of a large error in this factor on the calculated neutral point would amount to a fraction of a percent mean aerodynamic chord.

6. Summation of components

Figure 2 shows the variation of dC_m/dC_L with center-of-gravity position for the various components considered and from direct summation of the components for the airplane as a whole. The calculated stick-fixed neutral point is at 40.4 percent mean aerodynamic chord, the center-of-gravity position at which the value of dC_m/dC_L (total) is zero. The calculated neutral point is in good agreement with the flight value of 39.3 percent mean aerodynamic chord for normal-force coefficients between 0.3 and 1.2.

In the flaps-down condition with engines idling at the higher end of the speed range (C_L = 0.8 to 1.2), where it could be assumed that q_t/q was 0.9 and the data of figure 5, reference 4, indicated that there was no shift of the aerodynamic center of the wing due to flap deflection, the calculated neutral point was 40.4 percent mean aerodynamic chord as it was in the gliding condition and the flight value varied from 40 to 41 percent mean aerodynamic chord.

B. Elevator trim curves

1. Gliding condition (engines idling, flaps up, landing gear up)

The variation of elevator deflection required for trim with indicated airspeed was calculated for center-of-gravity positions of 23 and 32 percent of the mean aerodynamic chord. The resultant pitching moment of the airplane about the specified center-of-gravity positions was determined at $C_L = 0$. A value of C_{m_o} of -0.03 for the wing was obtained

from figure 5, reference 4. The increments of pitching moment due to fuselage, tail, and idling propellers were obtained using the expression:

$$C_{m_{f,t,p}} = \left(\frac{dC_m}{dC_L}\right)_{f,t,p} \left(\frac{dC_L}{d\alpha}\right)_w \alpha$$

Values of dC_m/dC_L were obtained from figure 2. Using an estimated angle of zero wing lift of -2° and assuming the root incidence of 2° to be constant along the span gave an angle of attack of -4° for fuselage tail and propellers. The elevator deflection required at $C_L = 0$ was determined from the expression:

$$\delta_e = \frac{C_m}{\left(\frac{dC_L}{d\alpha}\right)_t} \frac{S}{S_t} \frac{q}{q_t} \frac{c}{l_t} \frac{1}{\tau}$$

Differentiation of this expression with respect to C_m yielded $d\delta_e/dC_m$ and multiplying $d\delta_e/dC_m$ by dC_m/dC_L gave $d\delta_e/dC_L$, the slope of the elevator trim curve. Figure 3 shows the flight and calculated variation of elevator angle with lift coefficient for center-of-gravity positions of 23 and 32 percent mean aerodynamic chord.

For further comparison with flight data the variation of elevator angle required for trim with speed was calculated assuming an airplane weight of 29,000 pounds. This weight was the approximate weight of the airplane during the flight tests. Figure 4 shows a comparison of the calculated and flight values. Good agreement was obtained throughout the speed range.

2. Landing condition (engines idling, flaps down, landing gear down)

An increment of lift coefficient ΔC_L of 0.95 due to 50° flap deflection was used in the calculation of flap-down elevator trim curves.

This increment was calculated by applying the elevator effectiveness factor of reference 6, figure 3, to estimate the change in angle of attack of the flapped portion of the wing excluding any fuselage or nacelle area. The assumption that the effect of the flaps did not carry across fuselage or nacelles tends to account for the loss in flap effectiveness due to the gaps about 4 inches wide between the flaps and nacelles and between the flaps and the fuselage. The expression used to calculate the increment of lift coefficient due to flap deflection was:

$$\Delta C_L = \Delta \delta_f \, \tau \, \frac{dC_L}{d\alpha} \, \frac{S_{flapped}}{S_w}$$

The flapped area of the wing as defined above was 260 square feet and the value of τ was 0.46. The data of figure 3, reference 4, obtained from two-dimensional tests of a double-slotted flap installation similar to that on the A-26B, showed a linear variation of effective angle of attack with flap deflection up to 45° beyond which angle the flap effectiveness gradually decreased. A value of τ determined from figure 3, reference 4, was of nearly the same magnitude as the value obtained from figure 3, reference 6, used in the calculations. Wind-tunnel tests of a model of the A-26 airplane gave the same increment of trimmed lift coefficient as the above calculations. Figure 5 shows the variation of lift coefficient with angle of attack with flaps up and flaps down.

The data of figure 5, reference 4, showed that the wing aerodynamic center did not shift with flap deflection over a considerable portion of the lift-coefficient range. The pitching moment due to deflecting the flaps fully was determined by two different methods. An increment of pitching-moment coefficient of -0.338 was obtained by using the section pitching-moment data of figure 5, reference 4, and the method of reference 9 for determining the pitching-moment coefficient of a wing with a partial-span flap. The pitching moment due to deflecting the flaps was also obtained by assuming the increment

of lift coefficient, $\Delta C_L = 0.95$, to act at 50 percent of the mean aerodynamic chord. The pitching-moment increment was then equal to $-0.25\Delta C_L$ or -0.238.

The effect of the lowered landing gear was not included in the calculated values of elevator deflection for trim. However, it was estimated from the data of figures 19 and 20, reference 11, that approximately 1° up-elevator deflection would be required to counteract the pitching moment due to the landing gear. This value would vary somewhat with speed. It was found from flight data at 135 miles per hour that 1.1° more up elevator deflection was required for trim when the landing gear was lowered.

The elevator trim curves for the flap-down condition were calculated by the same method used for the flap-up condition. The downwash at the tail with the flaps deflected was obtained from figure 5, reference 10. Figure 6 presents the variation of elevator deflection for trim with lift coefficient for center-of-gravity positions of 21 and 30 percent mean aerodynamic chord obtained from flight and from the calculations using two values of pitching-moment increment due to flap deflection. Figures 7 and 8 present a comparison of flight and calculated curves of elevator deflection with flaps deflected against airspeed. The curves calculated from section flap pitching-moment data were offset somewhat from the flight data. Recalculating the pitching moment due to the flaps by the second, approximate method eliminated most of the offset. At speeds above which there was no flow breakdown over the wing in flight the calculated and flight curves have approximately the same slope. However, at low speeds the wing root stalled reducing the downwash at the tail and increasing the elevator deflection required in flight more rapidly than the calculated value increased.

C. Tail angle of attack

To determine whether there was any possibility of tail stalling, the maximum angle of attack of the horizontal tail was calculated. The critical condition was shown by calculations to be with the flaps down at

the maximum permissible speed, 160 miles per hour. With the flaps up, the angle of attack of the thrust axis and of the horizontal tail at zero lift would be approximately -4° as shown in figure 5. Lowering the flaps fully without changing the angle of attack would make the lift coefficient equal 0.95. The increment of downwash at the tail due to full deflection of the flaps was estimated from figure 5, reference 10, to be -5.1°. The resultant angle of attack of the tail at $C_L = 0.95$ with flaps down would be -9.1°. The change in true angle of attack of the tail going from $C_L = 0.95$ to $C_L = 0.81$, which corresponds to 160 miles per hour, was approximately -1° resulting in an angle of attack of the tail of approximately -10° not including the effect of propellers. Idling propellers would reduce this angle very slightly, but with power on it would be increased. No estimate was made of the increase in downwash angle due to application of power. In flight tests there was no indication of tail stalling.

D. Elevator deflection required for landing

The elevator deflections required to hold the airplane in the landing attitude near the ground have been calculated by the method of reference 9. The landing attitude angle measured with respect to the thrust axis was considered to be 8° which would correspond to an angle of attack of 8° at zero rate of descent and (from fig. 5) to a lift coefficient of 2.0. Figure 9 shows a comparison of flight and calculated values of the variation of elevator angle required to land with center-of-gravity position. Because of the root stall on the wing and the resulting decrease in downwash over the tail it had been expected that the calculated deflections would be less than those from flight data. However, the only two flight points which lie above the calculated curve were from landings during which additional elevator control was used for rapid flaring.

E. Minimum speed to raise nose wheel

The minimum speed to raise the nose wheel for take-off was determined by a summation of moments about the main wheels including the inertia forces acting on the airplane. The moments due to the weight of the airplane, the tail lift with fully deflected elevators, the resultant force along the thrust axis, and the wing lift

were considered. It was assumed that the resultant drag force acted through the center of gravity. A tire friction coefficient of 0.04 was used. A process of successive approximations was required in the calculations. It was determined from momentum calculations that $\frac{q_t}{q} \approx 2$ at the minimum speed for raising the nose wheel. Figure 10 is a plot of calculated values and those estimated by the pilot against center-of-gravity position. The calculated results are somewhat conservative.

F. Maneuvering stability and control

Stick-fixed neutral points for turning flight or stick-fixed maneuver points were calculated for constant speed turns at 235 miles per hour at sea level and at 10,000 feet altitude. The increment of elevator deflection due to turning was calculated from the formula:

$$\Delta\delta_e = \frac{\Delta C_L \rho g l_t}{2\tau \frac{W}{S}} \left(1 + \frac{1}{n}\right)$$

where ΔC_L is increase in lift coefficient from straight flight at the desired speed. The increment of elevator angle due to turning was added to the elevator angle required for trim in steady flight (fig. 3) at the same lift coefficient. If the tail length is assumed constant for all center-of-gravity locations (the allowable center-of-gravity movement is small compared to the tail length), the increment of elevator angle due to turning is a constant for all center-of-gravity locations. Figures 11 and 12 show the variation of elevator angle with lift coefficient in constant-speed turns at 235 miles per hour at 0 and 10,000 feet altitude and center-of-gravity locations of 23 and 32 percent mean aerodynamic chord. The stick-fixed neutral points in turning flight were determined at 2g at 235 miles per hour at sea level and at 10,000 feet by measuring the slopes of the curves of figures 11 and 12 and plotting the values of $d\delta_e/dC_L$ against center-of-gravity location. Figure 13 shows these plots. Flight data showed the stick-fixed neutral point in a 2g turn with rated power at 235 miles per hour and approximately 10,000 feet altitude to be at 43.3 percent mean aerodynamic chord. The calculated

value of neutral point for the same condition is 45.6 percent mean aerodynamic chord. It is permissible to compare the neutral point measured in turning flight using rated power with the calculated value for turns in the gliding condition because the thrust coefficient was small at the moderately high speed under consideration and does not vary with acceleration. The effect of power on longitudinal stability should be small in turns at 235 miles per hour but some of the discrepancy between the calculated and flight neutral points can be charged to the destabilizing effects of power.

II. Directional Stability and Control

A. Directional stability, rudder fixed

The directional stability of the airplane with engines idling was calculated by summing up the variation of yawing-moment coefficient with angle of yaw, $dC_n/d\beta$, for the various components of the airplane. For all directional-stability calculations it was assumed that q_t was equal to $0.9q$ and no account has been taken of sidewash. The assumption that sidewash could be neglected which simplified the calculationsis believed to be justified because the vertical tail is relatively far removed from the influence of the wing and fuselage and is not in the propeller slipstream.

1. Contribution of vertical tail

The contribution of the vertical tail to directional stability was calculated from the following formula:

$$\left(\frac{dC_n}{d\beta}\right)_t = \frac{dC_{N_t}}{d\beta} \times \frac{S_t q_t l_t}{Sqb}$$

$$= -0.00222$$

The value of the slope of the lift curve of the vertical tail used was 0.045 per degree obtained from figure 3, reference 12. As recommended in reference 12 the effective aspect ratio of the vertical tail was assumed to be 1.5 times the actual aspect ratio to take into account the end-plate effect of the horizontal tail.

2. Effect of idling propellers

The effect of idling propellers was obtained from the expression:

$$\left(\frac{dC_n}{d\beta}\right)_p = \frac{\pi l_p D^2 \left(\frac{dC_Y}{d\psi}\right)_p}{4Sb}$$

$$= 0.000072 \text{ per propeller per degree}$$

From figure 6, reference 8, $\left(\frac{dC_Y}{d\psi}\right)_p = 0.12$

3. Nacelle effect

An empirical formula which had been developed by Langley flight division personnel was used to estimate the nacelle effect.

$$\left(\frac{dC_n}{d\beta}\right)_n = 0.0158 \frac{S_n^2}{l_n Sb}$$

$$= 0.00018 \text{ per nacelle per degree}$$

4. Wing, fuselage, and interference effects

The contributions to the directional stability of the wing, fuselage, and wing-fuselage interference were estimated using data presented in reference 13 for the model with tapered midwing having 4.75° sweepback.

$$\left(\frac{dC_n}{d\beta}\right)_w = -0.00015$$

$$\left(\frac{dC_n}{d\beta}\right)_f = 0.0003$$

$$\left(\frac{dC_n}{d\beta}\right)_T = -0.0001$$

5. Effect of dorsal

The yawing-moment coefficients due to the dorsal fin at various sideslip angles were obtained from reference 14 using the data of figure 5 for a type 2 dorsal, which had the same relative size as the dorsal fin used on the A-26 airplane.

β	C_n
-5	-0.0006
-10	-0.0017
-15	-0.0033

Figure 14 shows the calculated variation of yawing-moment coefficient of the airplane with rudder fixed and engines idling.

B. Rudder deflection for trim

From the data of figure 14 and the formula:

$$\delta_r = \frac{C_{nSb}}{\frac{dC_{Nt}}{d\beta} \tau \frac{q_t}{q} S_t l_t}$$

the variation of rudder deflection with angle of sideslip was calculated. The value of the rudder effectiveness factor τ was found to be 0.6 from figure 4, reference 12. Figure 15 presents a comparison of flight and calculated values of the variation of rudder deflection with angle of sideslip for the clean condition with engines idling. The agreement between flight and calculated values is best at low angles of sideslip. The difference between the slopes of the calculated and test curves at the larger sideslip angles may be due to underestimation in the calculations of the effect of the dorsal fin at large sideslip angles.

C. Asymmetric power condition

1. Rudder deflection for trim at 0° sideslip

Calculations were made to determine the directional stability and control characteristics with

the left propeller inoperative and the right engine delivering normal-rated power. Figure 16 shows the calculated values of the variation with indicated airspeed of rudder deflection required to maintain zero sideslip. The rudder deflections were calculated from the formula

$$\delta_r = \frac{\text{bhp } \eta \text{ a } \frac{550}{V}}{\left(\frac{dC_{N_t}}{d\beta}\right) \tau \, q_t \, S_t l_t}$$

where the numerator is the yawing moment due to asymmetric power and the denominator is the yawing moment per degree of rudder deflection. The propeller efficiency η was determined from figure 3-13, reference 15, for the various propeller advance-diameter ratios and q_t was assumed to be 0.9q.

Flight data were available from runs made with the wings level in which there was a small amount of sideslip. The accuracy of the calculated data in figure 16 is indicated by the close agreement between rudder deflections used in flight and calculated values of rudder deflections required to trim at the angles of sideslip held in flight.

2. Sideslip with rudder fixed

Figure 17 shows the variation with speed of the sideslip angle required during single-engine operation with the rudder fixed in neutral. This curve was obtained by first determining the yawing-moment coefficient C_n required to balance the yawing moment due to asymmetric thrust by the formula

$$C_n = \frac{\text{bhp } \eta \text{ a } 550}{qSbV}$$

and then from figure 14 determining the sideslip angle at which the required value of C_n is reached.

Flight data were available from runs made with the rudder free. The variation of angle of sideslip

with indicated airspeed was calculated using rudder trailing angles from the flight data. Figure 17 shows very close agreement between actual and calculated sideslip angles with a given rudder trailing angle.

3. Rudder deflection for trim as a function of sideslip angle

Figure 18 shows the rudder deflection required for trim during single-engine operation as a function of sideslip angle at indicated airspeeds of 120 and 140 miles per hour. These curves were calculated from the formula

$$\delta_r = \frac{\text{bhp } \eta \text{ a } \frac{550}{V} - C_n q S b}{\left(\frac{dC_{N_t}}{d\beta}\right) \tau q_t S_t l_t}$$

where the numerator is the difference between the yawing moment due to asymmetric power and the airplane restoring moment and the denominator is the yawing moment per degree of rudder deflection. The value of C_n in the above formula was obtained from figure 14 for the sideslip angles at which the rudder deflection for trim was to be determined.

III. Lateral Control Characteristics

The aileron effectiveness $pb/2V$ was estimated by the method given in reference 16 using the formula:

$$\frac{pb}{2V} = \left(\frac{C_{l_\delta}}{K}\right) \frac{K\Delta\delta_a}{114.6\, C_{l_p}}$$

$\frac{C_{l_\delta}}{K}$ and C_{l_p} were obtained from reference 16 and a value of $K = 0.4$ was estimated from flight data presented in reference 17 for an airplane having 19-percent-chord cusped ailerons with 0.48 to 1 balancing tabs.

For a total aileron deflection of 34° with 0.36 to 1 balancing tabs, the aileron effectiveness pb/2V was calculated to be 0.078. The change in aileron effectiveness caused by varying the balancing tab ratio can be estimated by considering the tabs to be small ailerons and applying the above method. The value of K used for the balancing tabs would be approximately 0.15. The calculated value of aileron effectiveness was considerably higher than the value of $\frac{pb}{2V} = 0.063$ obtained in flight with the same aileron deflection. In making these calculations no account was taken of wing twist which would tend to reduce aileron effectiveness.

CONCLUSIONS

Regarding the comparison of predicted and actual flying qualities of the A-26B airplane the following statements can be made:

1. It was possible to predict within 1 percent mean aerodynamic chord the stick-fixed neutral point for the engines-idling condition with flaps up or down except in the flaps-down condition at low speeds $C_L > 1.2$ where the ratio of dynamic pressure at the tail to free-stream dynamic pressure and the downwash at the tail were not readily estimated.

2. It was possible to predict within 0.5° the elevator deflections required for trim in the gliding condition up to a lift coefficient of approximately 1.2 where root stall of the wing occurred.

3. It was possible to predict by an approximate method the elevator deflections required for trim in the engines-idling, flaps-down condition to within 1° up to a lift coefficient of 1.4.

4. Calculations showed that no tail stall should occur with flaps down, power off, and no tail stall occurred in flight.

5. The predicted and actual elevator deflections required for landing were in very good agreement. However, it would be expected that the calculated

elevator deflections would be lower than the flight values because of the root stall which occurred in flight.

6. The predicted minimum speeds for raising the nose wheel were about 10 miles per hour higher than the measured speeds.

7. The predicted stick-fixed maneuver point for constant-speed turns at an indicated airspeed of 235 miles per hour with engines idling was about 2 percent aft of the maneuver point for power on flight. Some of the discrepancy can be charged to the destabilizing effect of power. The predicted elevator deflections for trim at various lift coefficients in a constant-speed turn with engines idling were about 1.5° more than deflections required in flight for power-on turns at the same speed.

8. It was possible to predict for the engines-idling, flaps-up condition the rudder deflection required for trim at a given angle of sideslip within 1° for angles of sideslip up to 10° above which the error increased probably due to underestimation of the stabilizing effect of the dorsal fin. The calculations were simplified in the case of the A-26 because the vertical tail was out of the slipstream and was relatively far removed from the influence of the wings and fuselage. Therefore, it was justifiable to neglect the effects of sidewash.

9. It was possible to predict within 2° the rudder deflection required for trim at any speed at 0° sideslip with one engine delivering full power and the other engine idling in the flaps-up condition.

10. It was possible to predict within 1.5° the angle of sideslip required for trim at any speed with the rudder fixed in the flaps-up condition with one engine delivering full power and the other engine idling.

11. The predicted aileron effectiveness $pb/2V$ was approximately 20 percent high. Wing twist which was not considered would tend to account for this discrepancy.

12. The results presented in this report indicate that many of the control-fixed, power-off stability and control characteristics of a conventional airplane can be predicted from the dimensions of the airplane and

from general wind-tunnel data now available with sufficient accuracy for design purposes.

Langley Memorial Aeronautical Laboratory
National Advisory Committee for Aeronautics
Langley Field, Va.

REFERENCES

1. Crane, H. L., Sjoberg, S. A., and Hoover, H. H.: Measurement of Flying Qualities of a Douglas A-26B Airplane (AAF No. 41-39120). I - Longitudinal Stability and Control Characteristics. NACA MR No. L4L06, 1944.

2. Sjoberg, S. A., Crane, H. L., and Hoover, H. H.: Measurement of Flying Qualities of a Douglas A-26B Airplane (AAF No. 41-39120). II - Lateral and Directional Stability and Control Characteristics. NACA MR No. L5A04, 1945.

3. Sjoberg, S. A., Crane, H. L., and Hoover, H. H.: Measurement of Flying Qualities of a Douglas A-26B Airplane (AAF No. 41-39120). III - Stalling Characteristics. NACA MR No. L5A04a, 1945.

4. Bogdonoff, Seymour M.: Wind-Tunnel Investigation of a Low-Drag Airfoil Section With a Double Slotted Flap. NACA ACR No. 3I20, 1943.

5. White, Maurice D.: Estimation of Stick-Fixed Neutral Points of Airplanes. NACA CB No. L5C01, 1945.

6. Gilruth, R. R., and White, M. D.: Analysis and Prediction of Longitudinal Stability of Airplanes. NACA Rep. No. 711, 1941.

7. Multhopp, H.: Aerodynamics of the Fuselage, NACA TM No. 1036, 1942.

8. Ribner, Herbert S.: Formulas for Propellers in Yaw and Charts of the Side-Force Derivative. NACA ARR No. 3E19, 1943.

9. Goranson, R. Fabian: A Method for Predicting the Elevator Deflection Required to Land. NACA ARR No. L4I16, 1944.

10. Silverstein, Abe, and Katzoff, S.: Design Charts for Predicting Downwash Angles and Wake Characteristics behind Plain and Flapped Wings. NACA Rep. No. 648, 1939.

11. Biermann, David, and Herrnstein, William H., Jr.: The Drag of Airplane Wheels, Wheel Fairings, and Landing Gears. II - Nonretractable and Partly Retractable Landing Gears. NACA Rep. No. 518, 1935.

12. Pass, H. R.: Analysis of Wind-Tunnel Data on Directional Stability and Control. NACA TN No. 775, 1940.

13. House, Rufus O., and Wallace, Arthur R.: Wind-Tunnel Investigation of Effect of Interference on Lateral-Stability Characteristics of Four NACA 23012 Wings, an Elliptical and a Circular Fuselage, and Vertical Fins. NACA Rep. No. 705, 1941.

14. Hoggard, H. Page, Jr.: Wind-Tunnel Investigation of Fuselage Stability in Yaw With Various Arrangements of Fins. NACA TN No. 785, 1940.

15. Millikan, Clark B.: Aerodynamics of the Airplane. John Wiley & Sons, Inc., 1941.

16. Gilruth, R. R., and Turner, W. N.: Lateral Control Required for Satisfactory Flying Qualities Based on Flight Tests of Numerous Airplanes. NACA Rep. No. 715, 1941.

17. White, Maurice D., and Hoover, Herbert H.: Flight Tests of Beveled-Trailing-Edge Ailerons with Various Modifications on a North American XP-51 Airplane (AAF No. 41-38). NACA MR, Dec. 7, 1943.

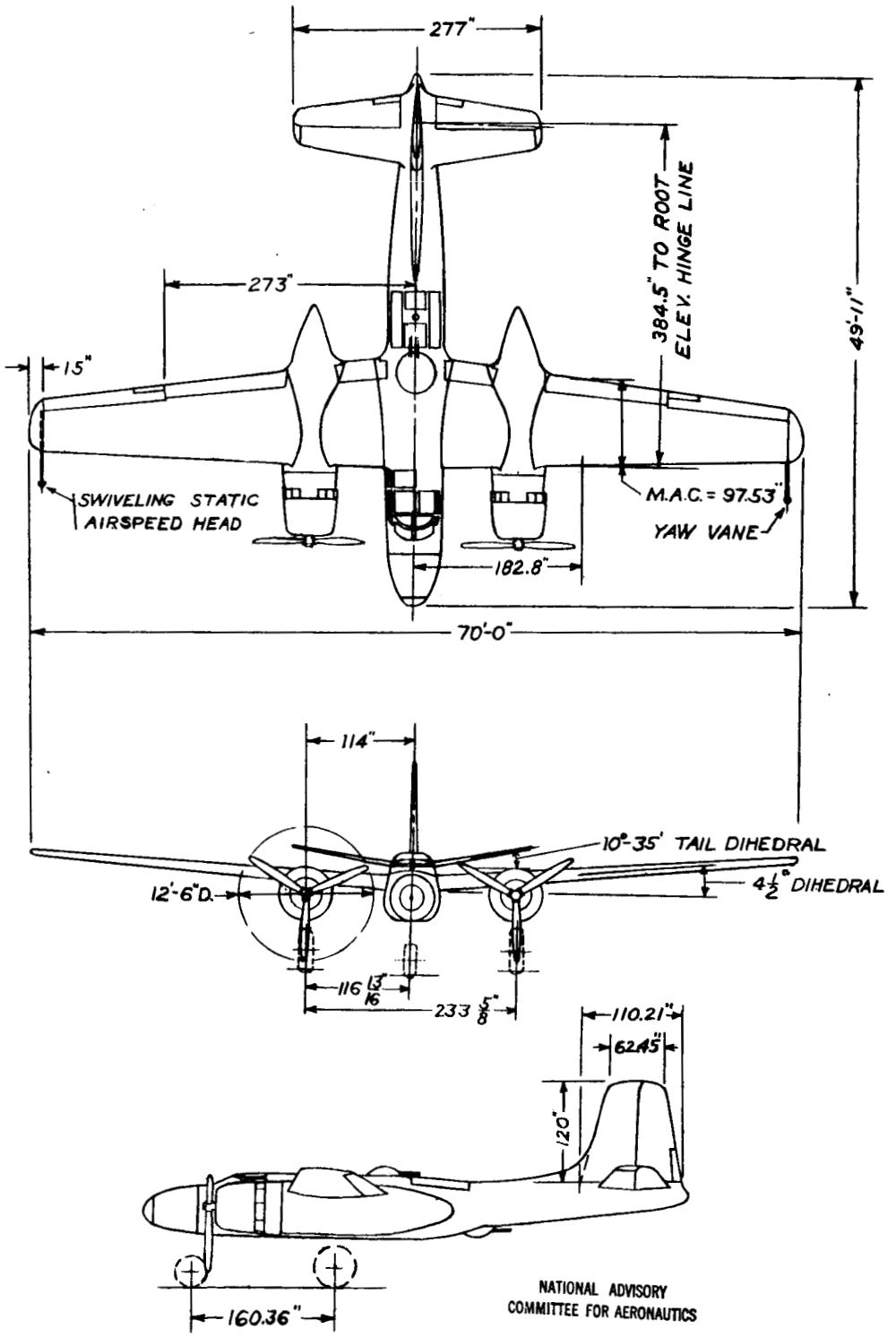

Figure 1. - Three-view drawing of the Douglas A-26B airplane.

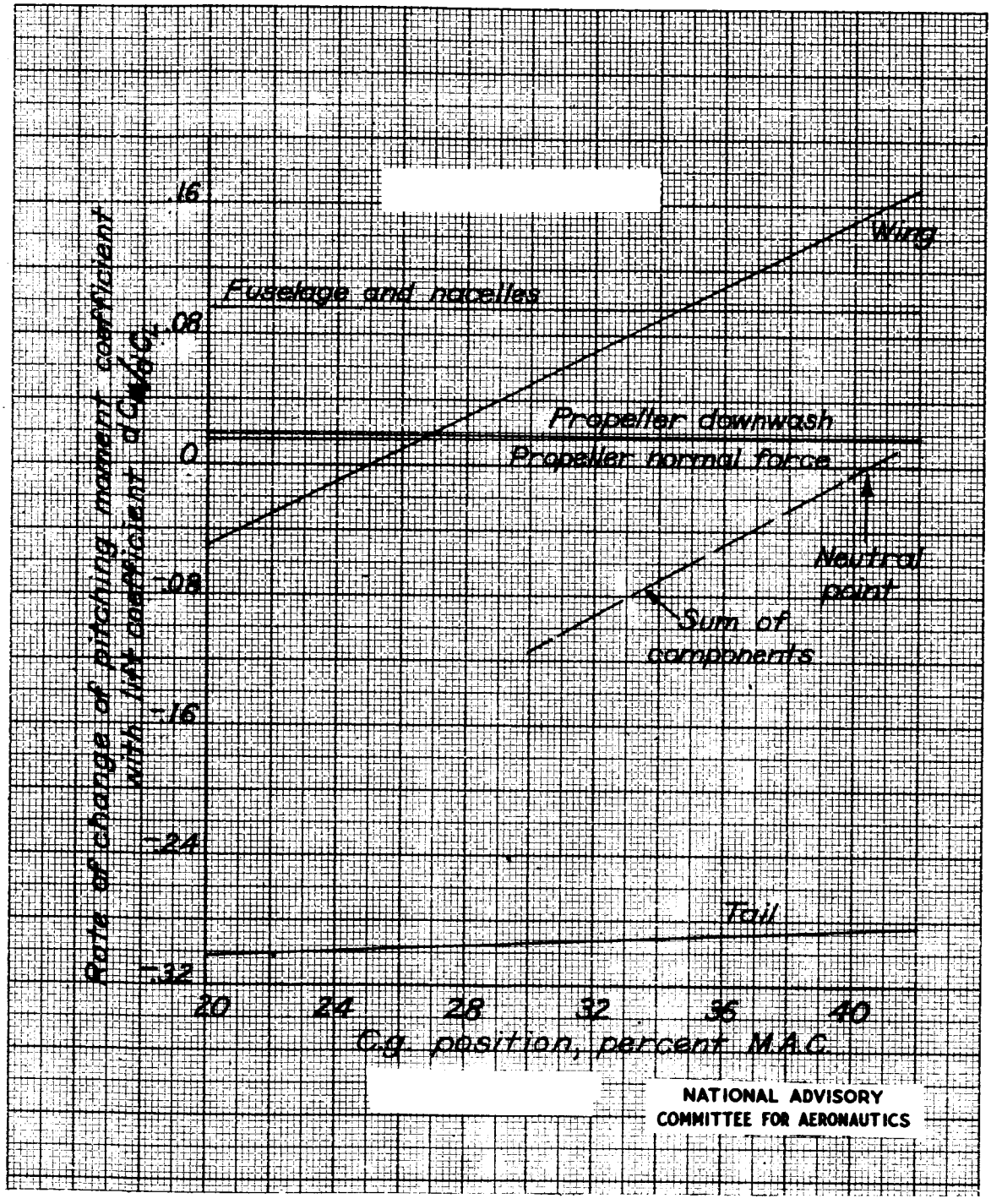

Figure 2. - Calculated variation of dC_m/dC_L with center-of-gravity position in the engines-idling, flaps-up condition, Douglas A-26B airplane.

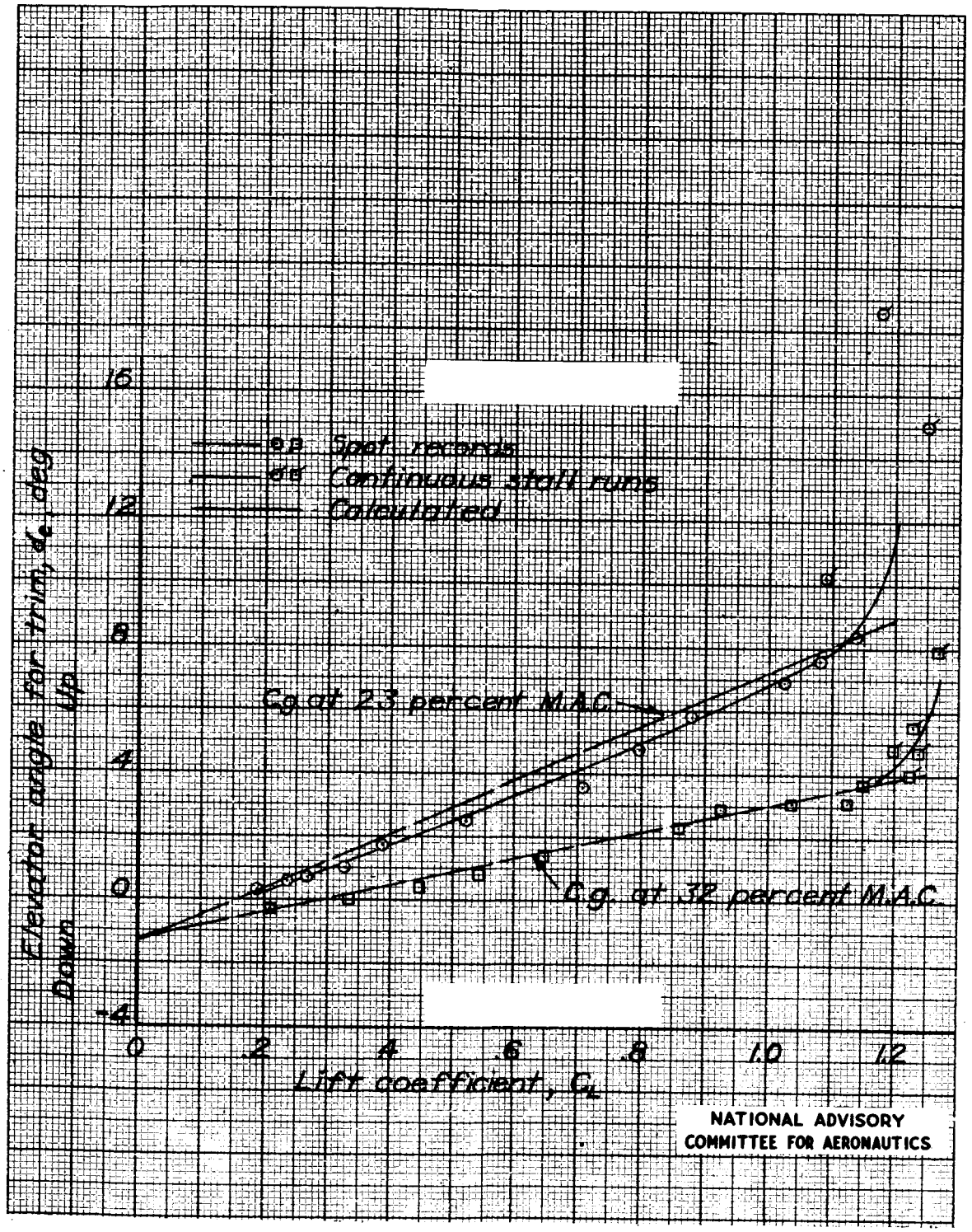

Figure 3. - Variation of elevator angle with lift coefficient for two center-of-gravity positions in the engines-idling, flaps-up condition, Douglas A-26B airplane.

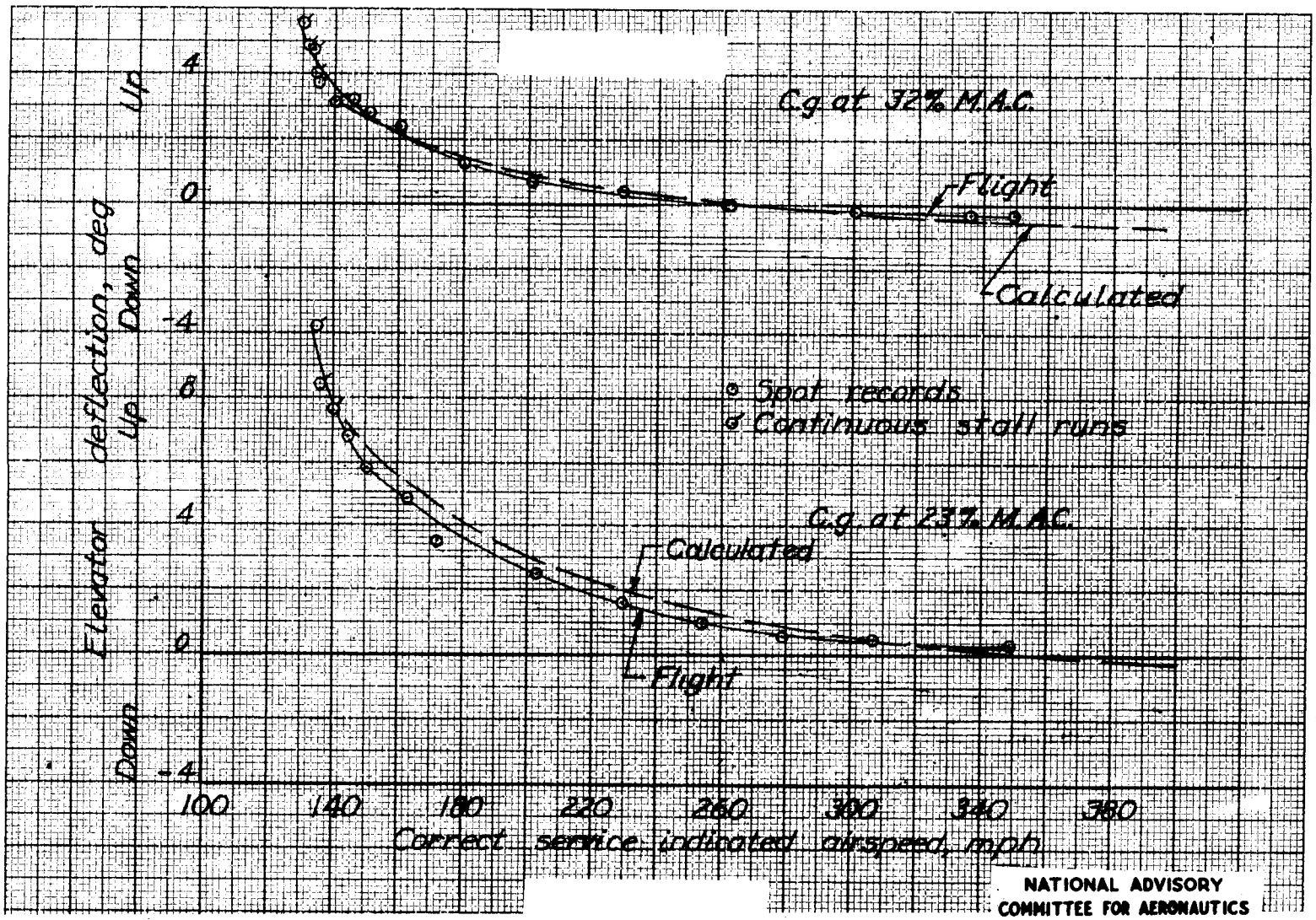

Figure 4. - Variation of elevator deflection with airspeed at two center-of-gravity positions in the engines-idling, flaps-up condition, Douglas A-26B airplane.

MR No. L5D06

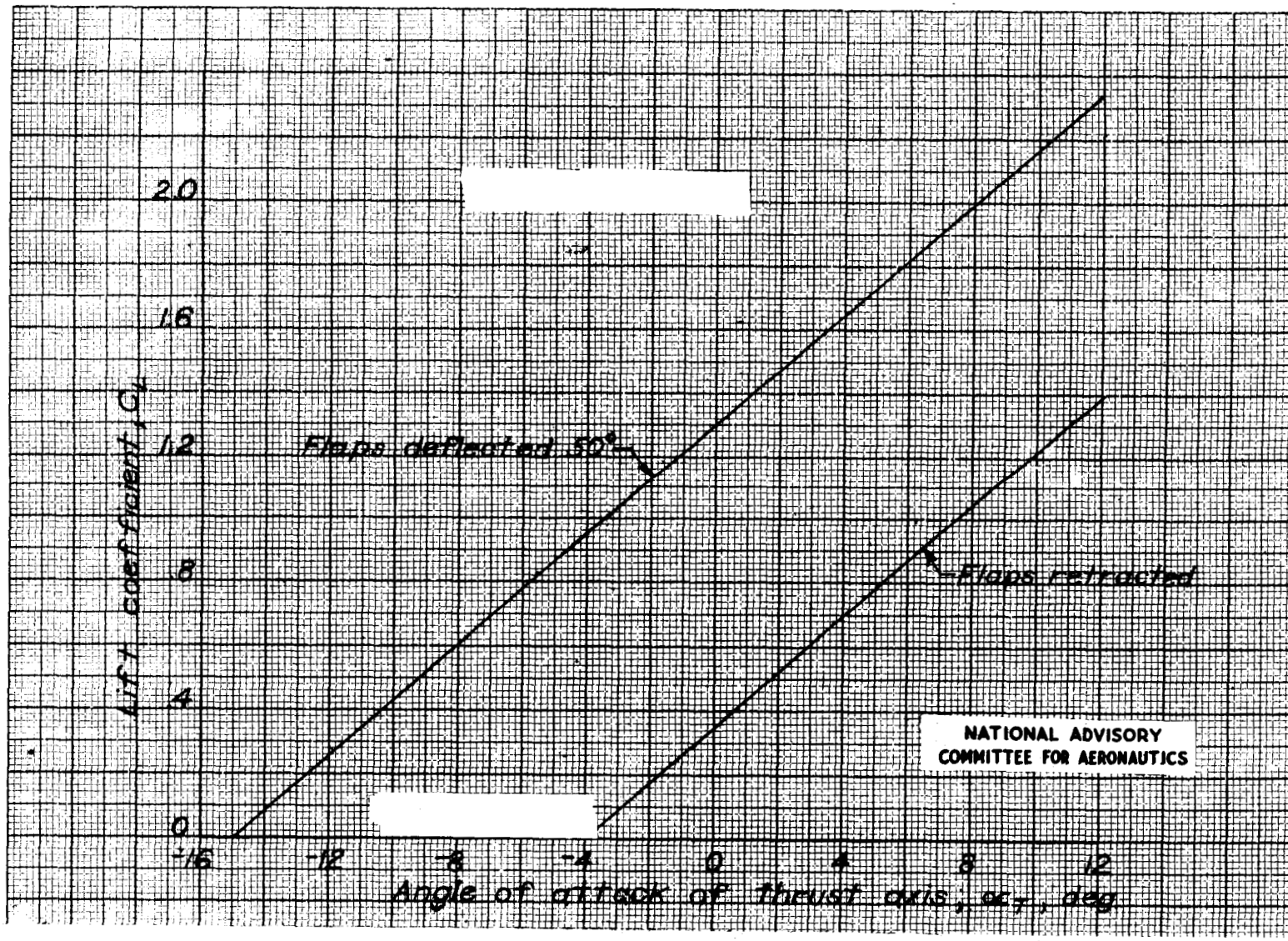

Figure 5. - Variation of lift coefficient with angle of attack, flaps up and flaps down, Douglas A-26B airplane.

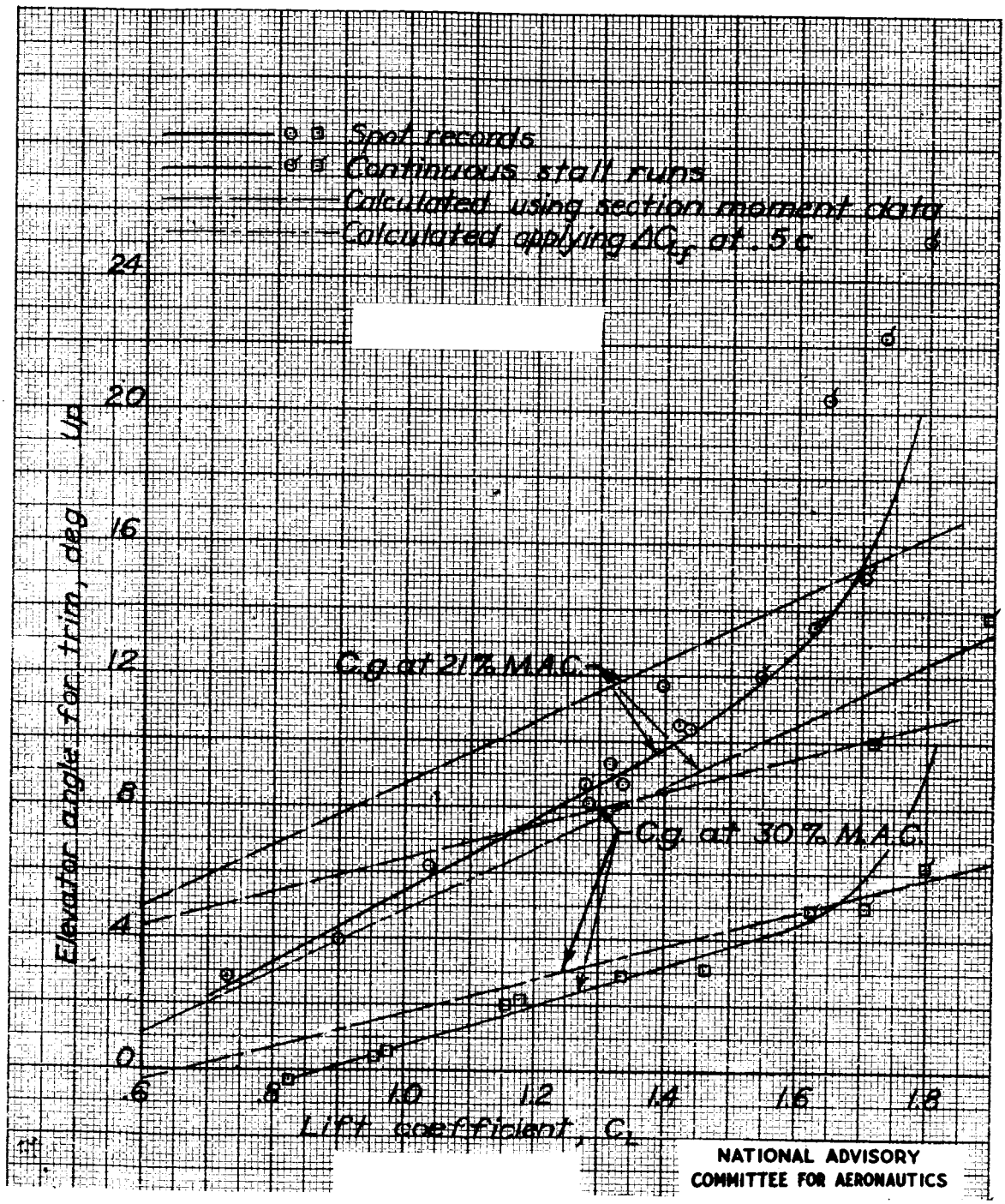

Figure 6. - Variation of elevator angle with lift coefficient for two center-of-gravity positions in the engines-idling, flaps-down condition, Douglas A-26B airplane.

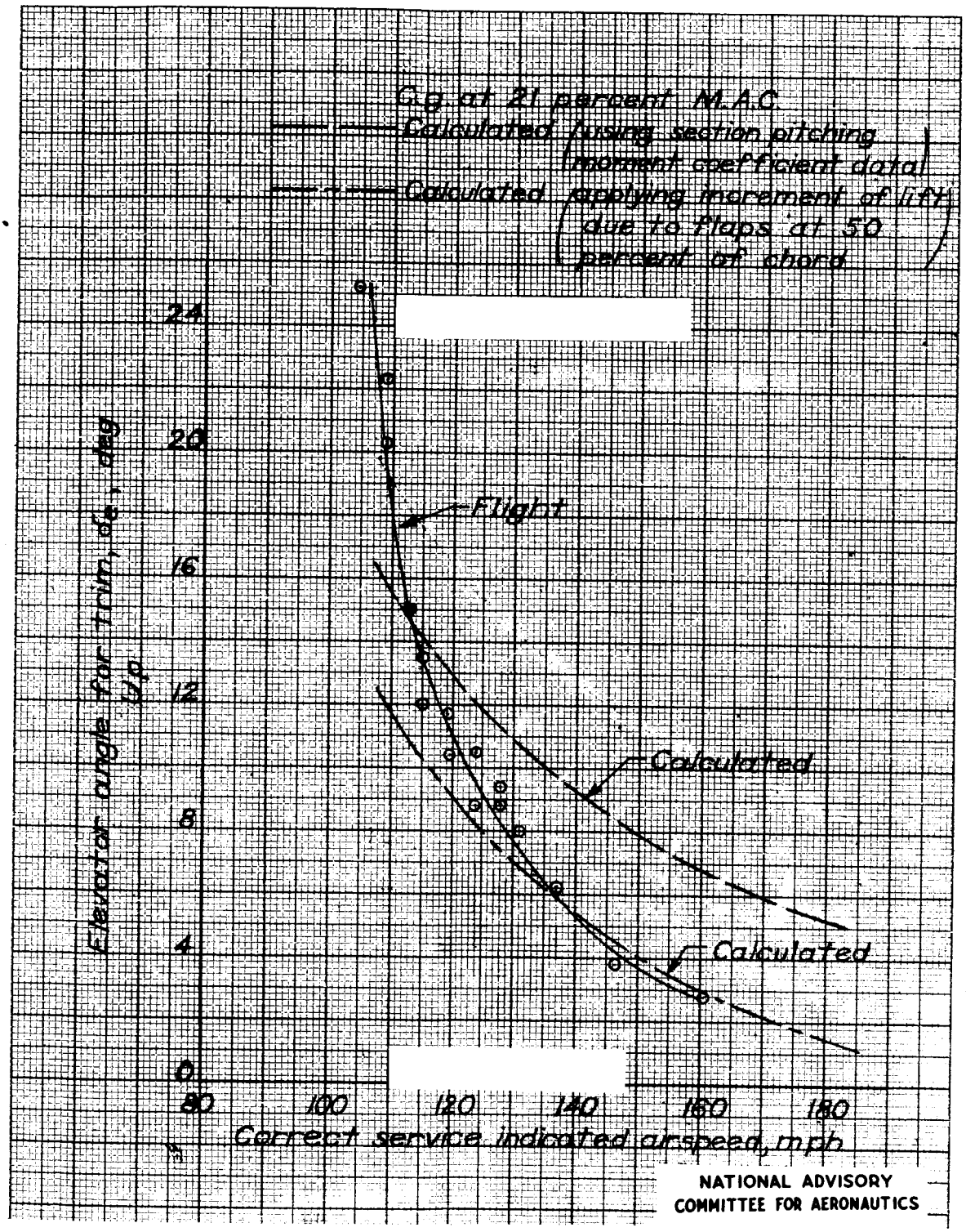

Figure 7. - Variation of elevator deflection with airspeed with the center of gravity at 21 percent M.A.C. in the engines-idling, flaps-down condition, Douglas A-26B airplane.

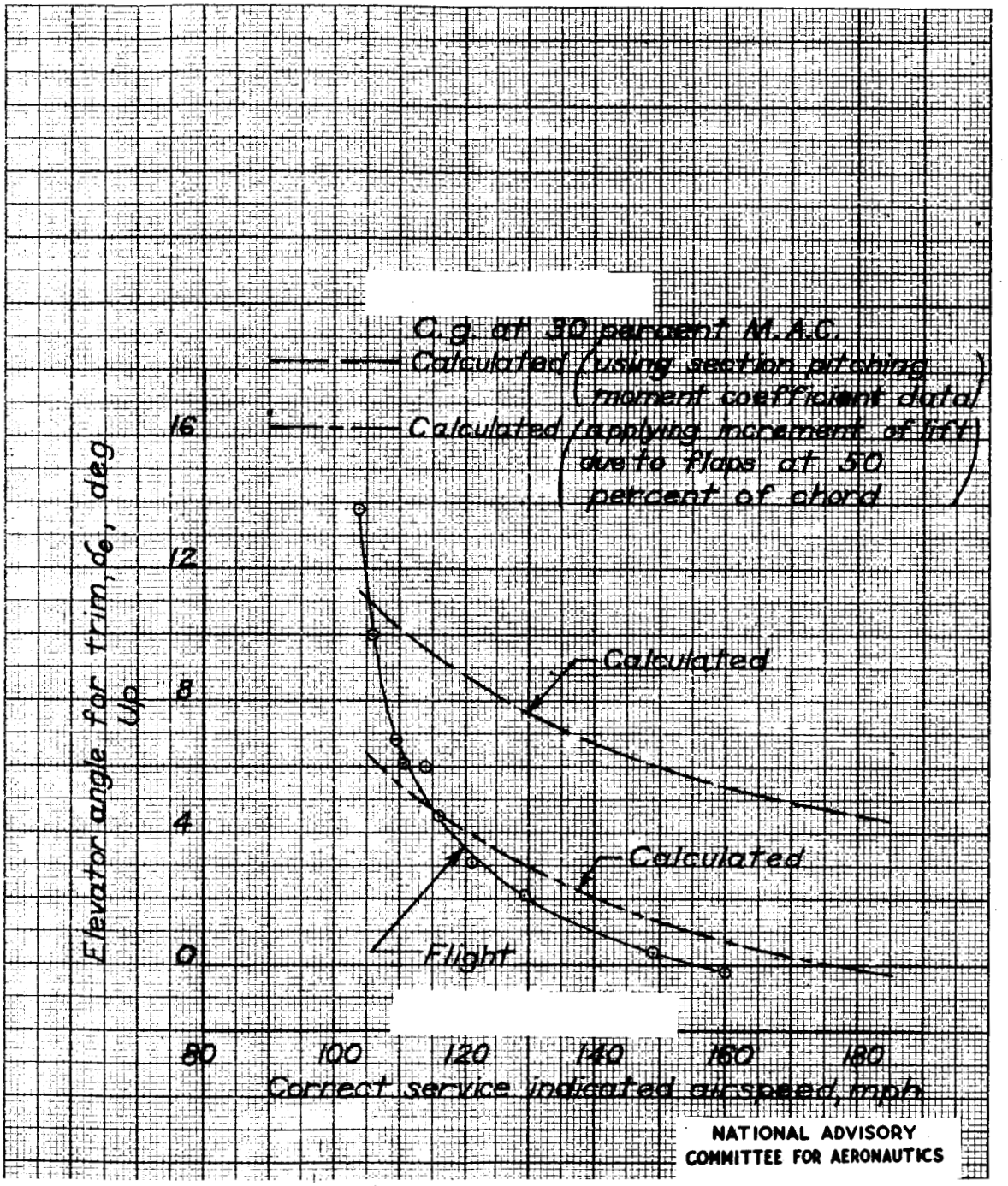

Figure 8. - Variation of elevator deflection with airspeed with the center of gravity at 30 percent M.A.C. in the engines-idling, flaps-down, Douglas A-26B airplane.

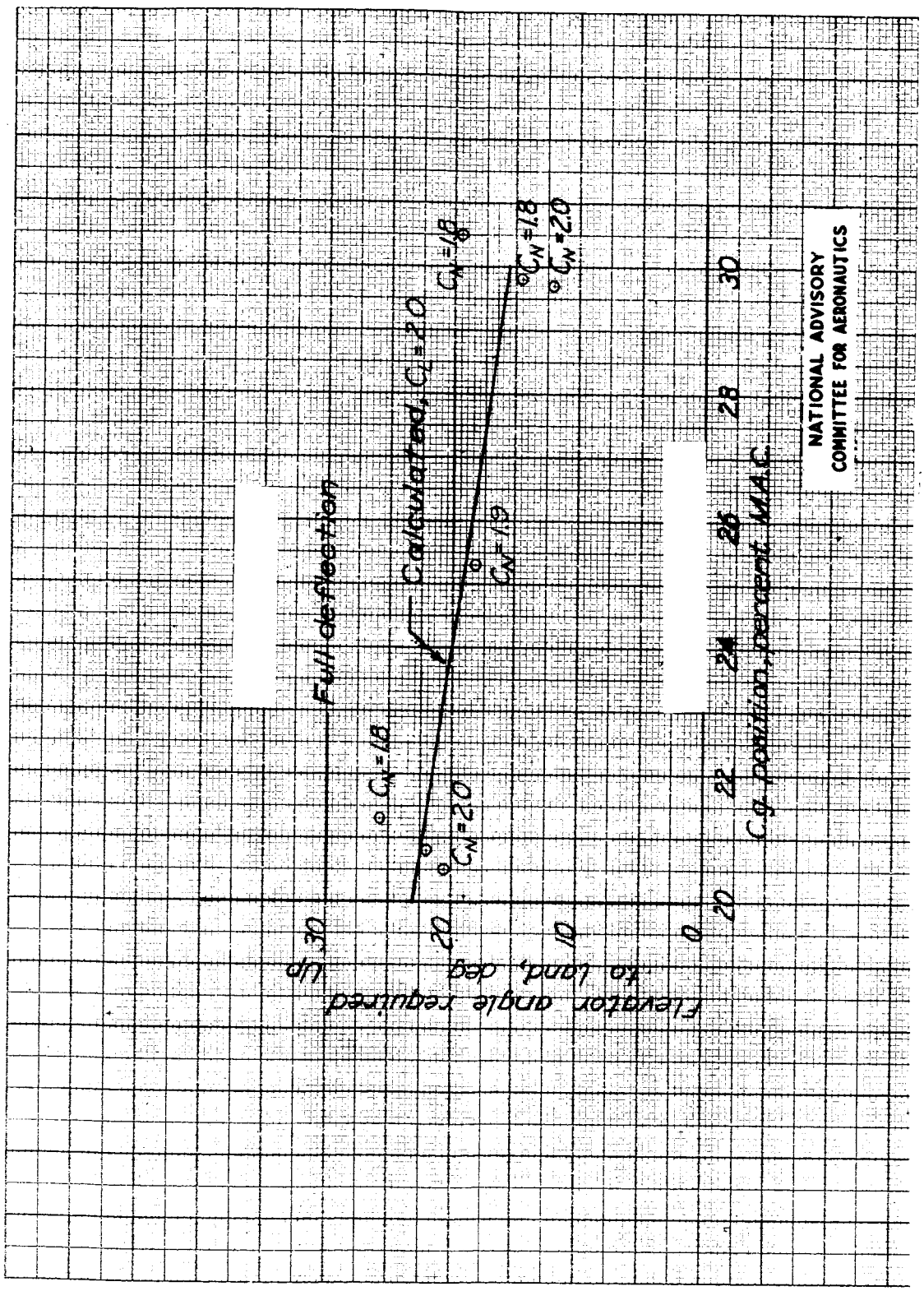

Figure 9. - Variation of elevator deflection required to land with center-of-gravity position in the engines-idling, flaps-down condition, Douglas A-26B airplane.

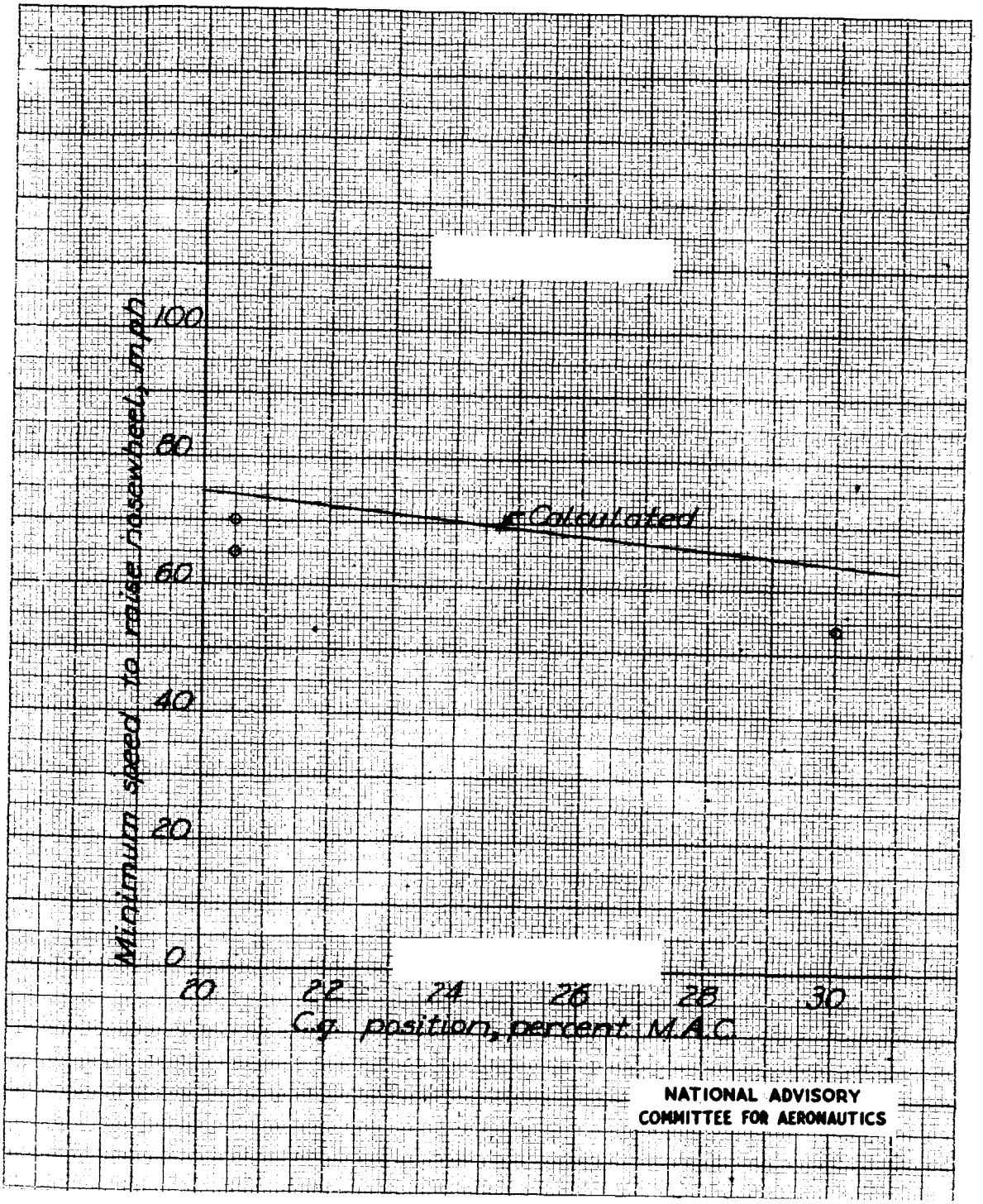

Figure 10. - Minimum speed to raise the nose wheel as a function of center-of-gravity position with take-off power and flaps down, Douglas A-26B airplane.

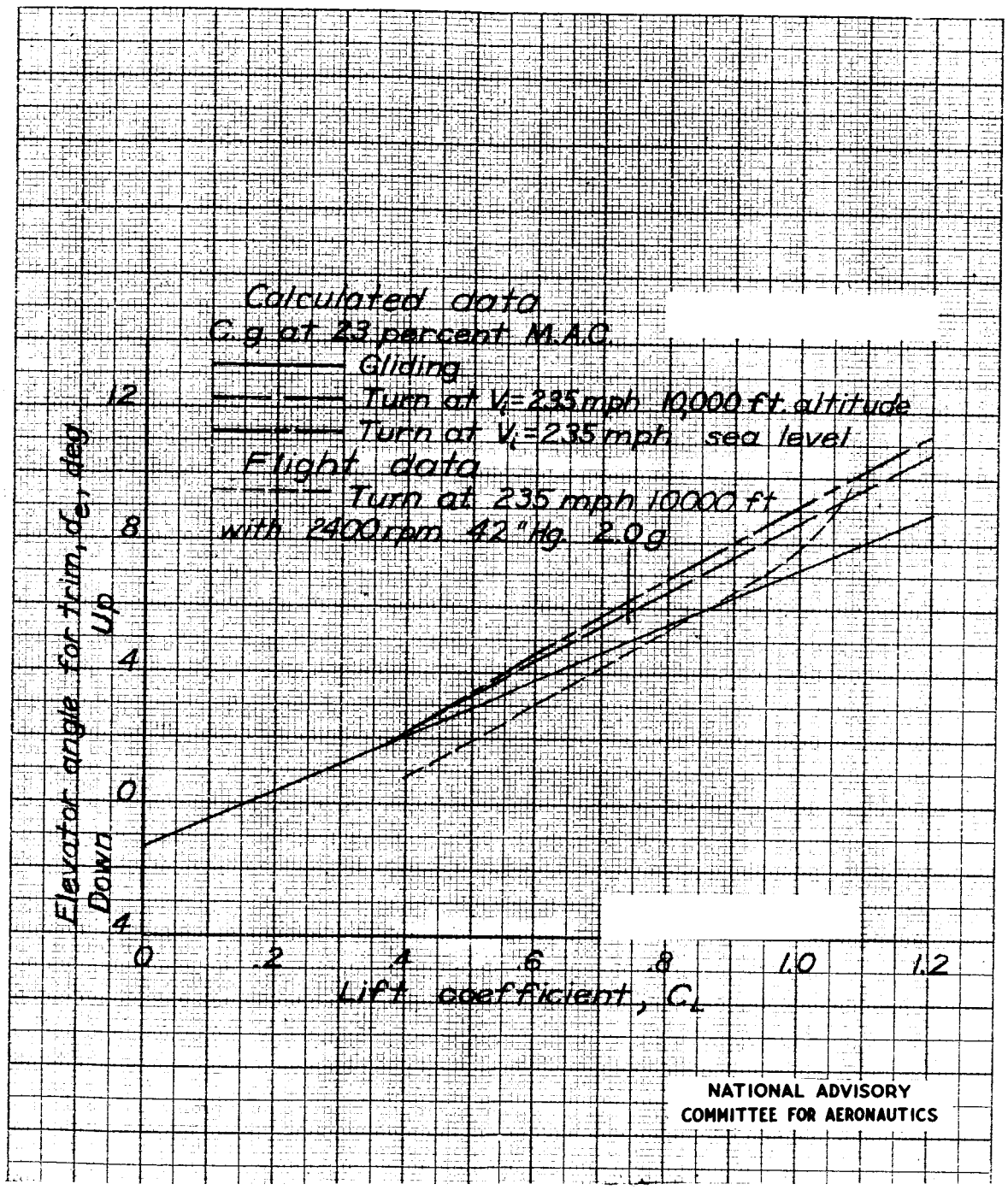

Figure 11. - Variation of elevator angle for trim with lift coefficient in turns at 235 miles per hour at sea level and 10,000 feet with the center of gravity at 23 percent M.A.C., engines idling, flaps up, Douglas A-26B airplane.

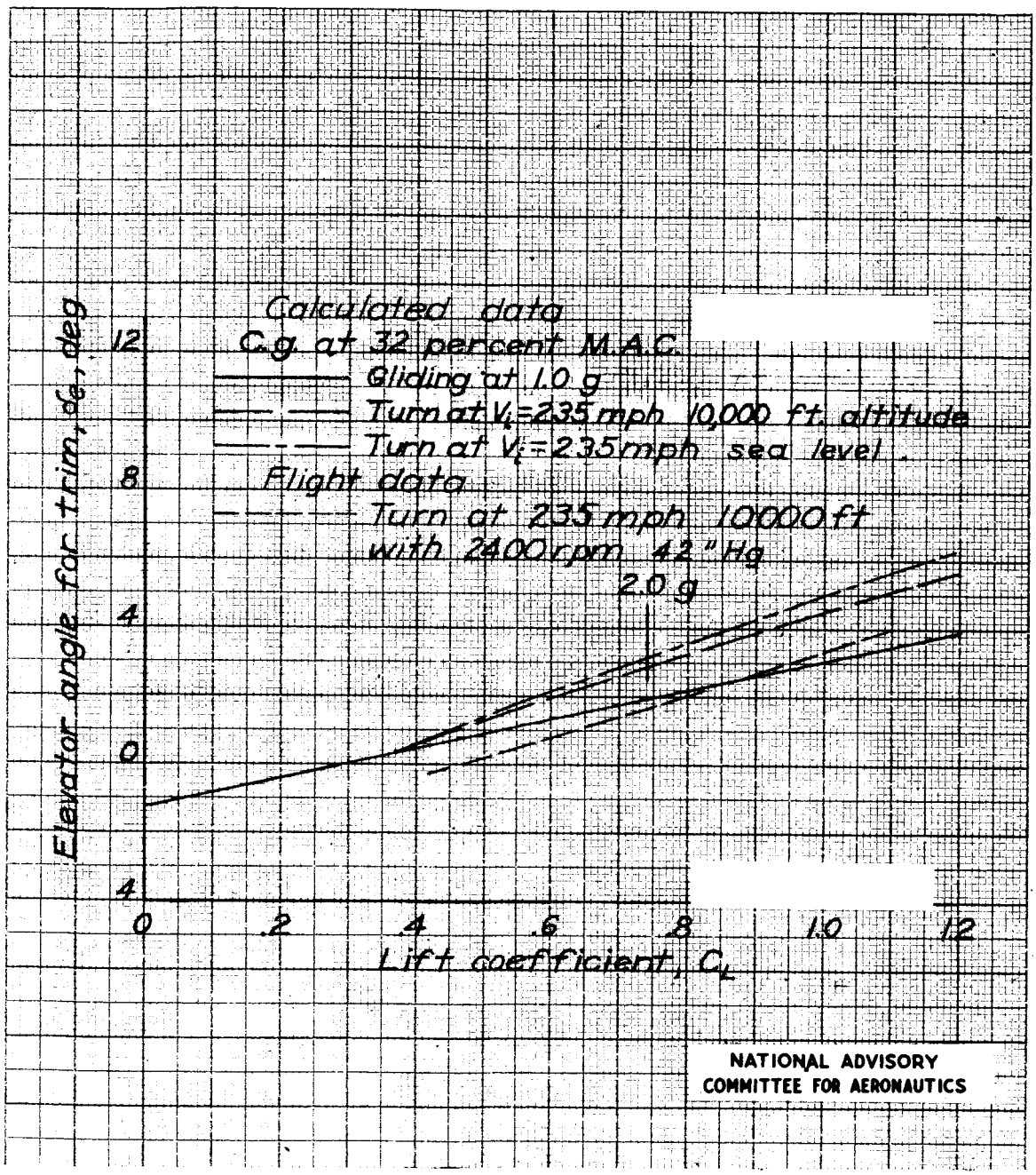

Figure 12. - Variation of elevator angle for trim with lift coefficient in turns at 235 miles per hour at sea level and 10,000 feet with the center of gravity at 32 percent M.A.C., engines idling, flaps up, Douglas A-26B airplane.

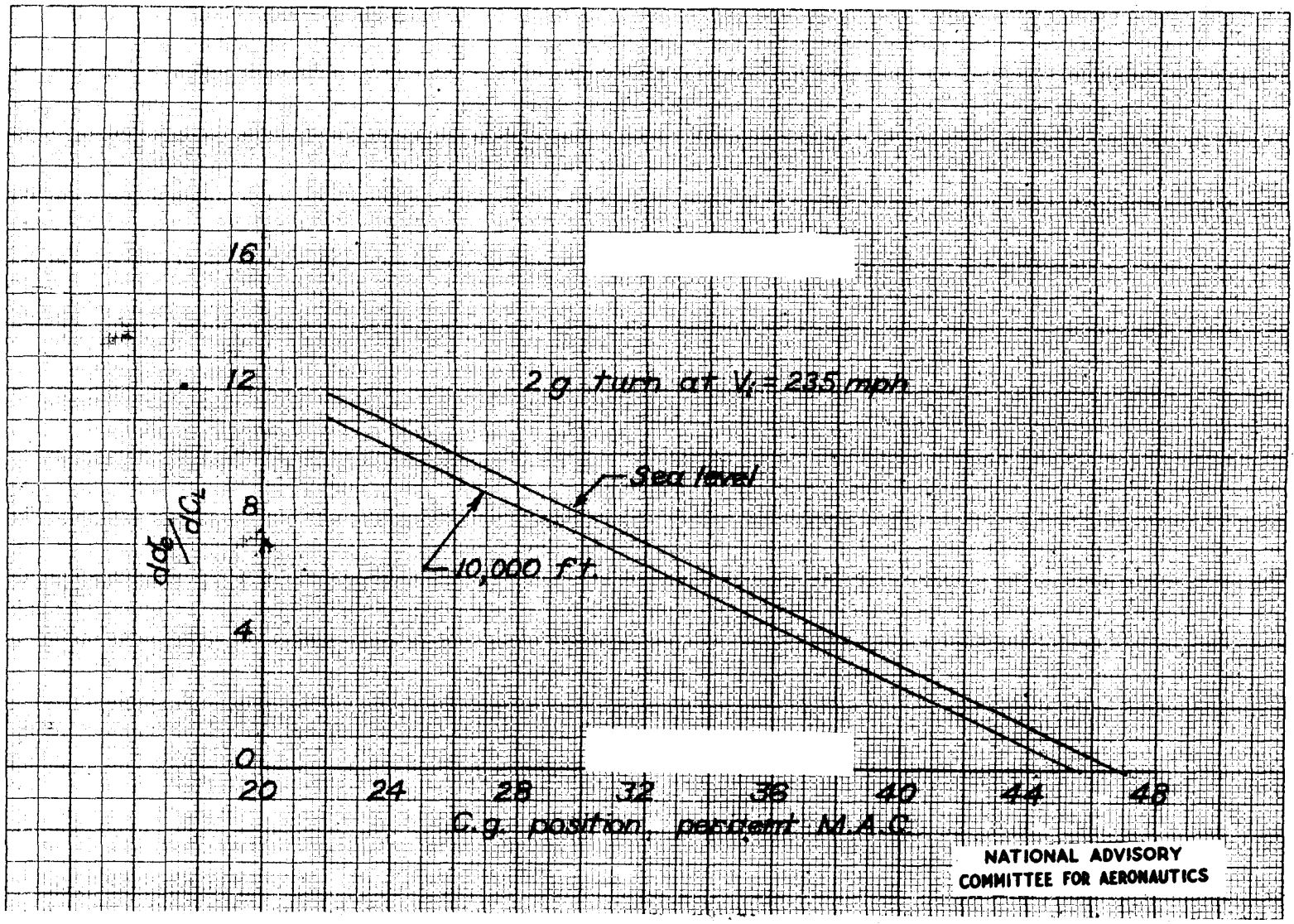

Figure 13. - Variation of $d\delta_e/dC_L$ with center-of-gravity position calculated for 2 g turns at sea level and 10,000 feet, engines idling and flaps up, Douglas A-26B airplane.

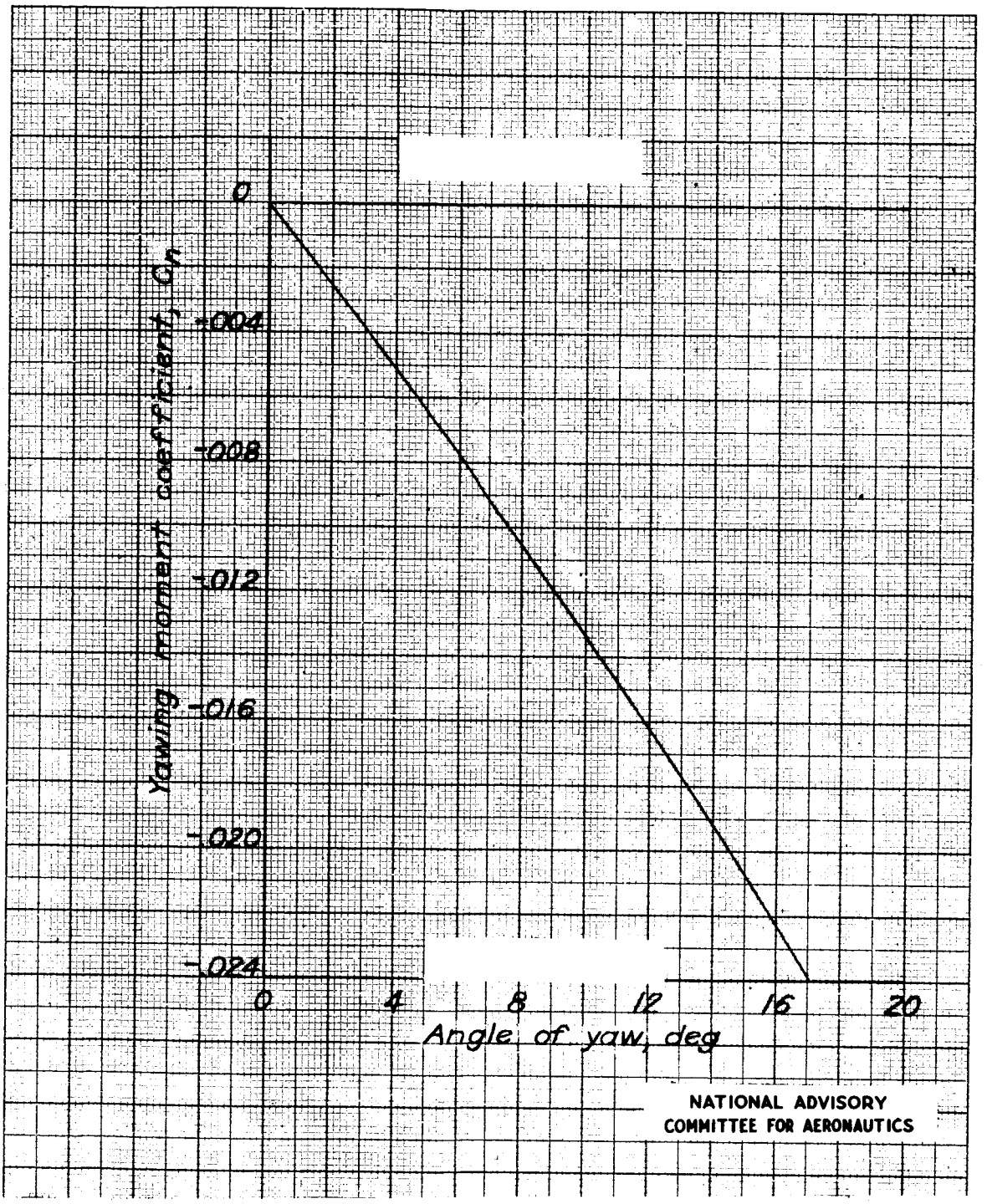

Figure 14. - Variation of yawing moment coefficient with angle of yaw, engines idling and flaps up, Douglas A-26B airplane.

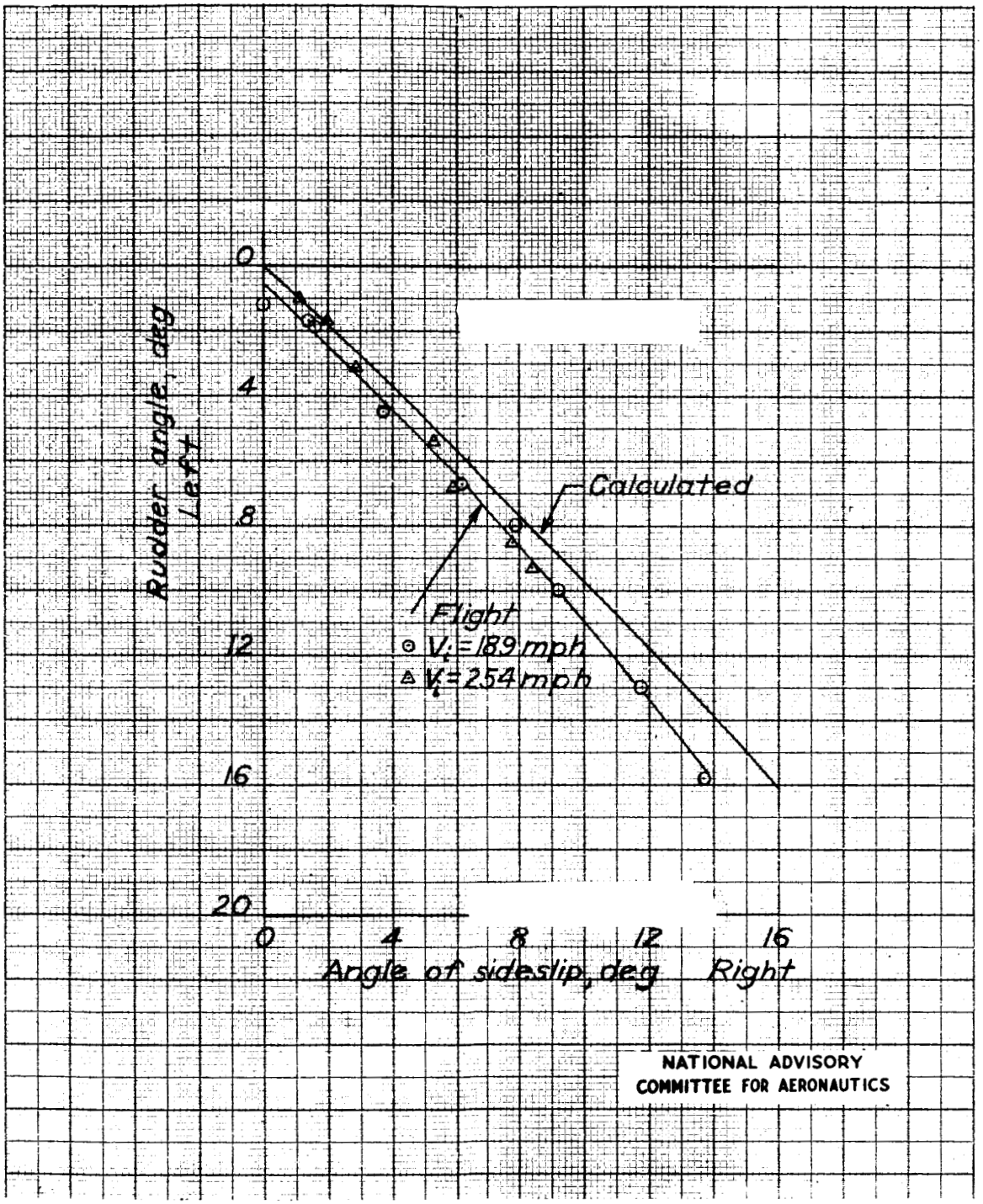

Figure 15. - Variation of rudder angle with sideslip angle in the engines-idling, flaps-up condition, Douglas A-26B airplane.

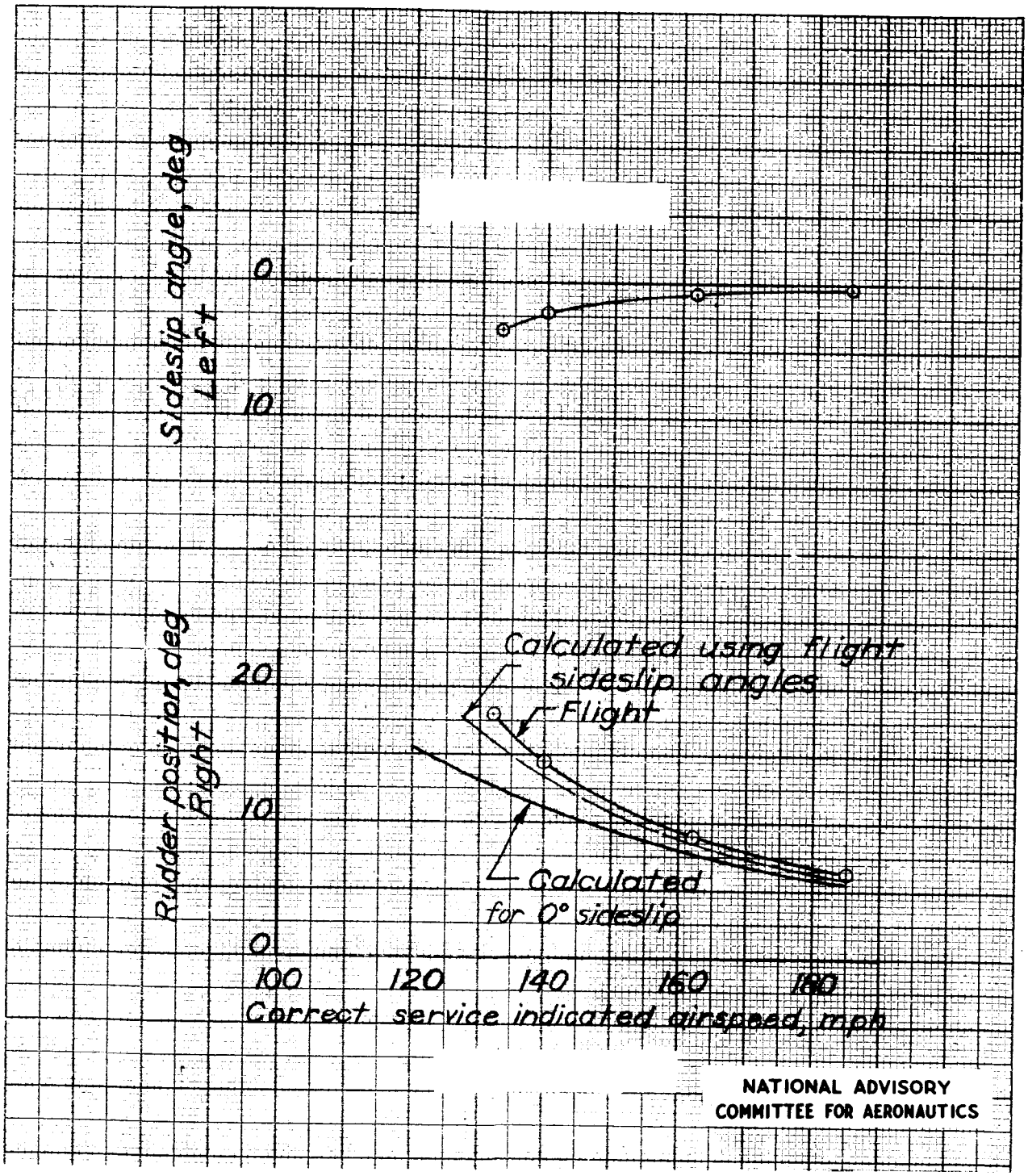

Figure 16. - Variation of rudder angle required for trim with airspeed with the left engine idling and right engine delivering rated power with the flaps up, Douglas A-26B airplane.

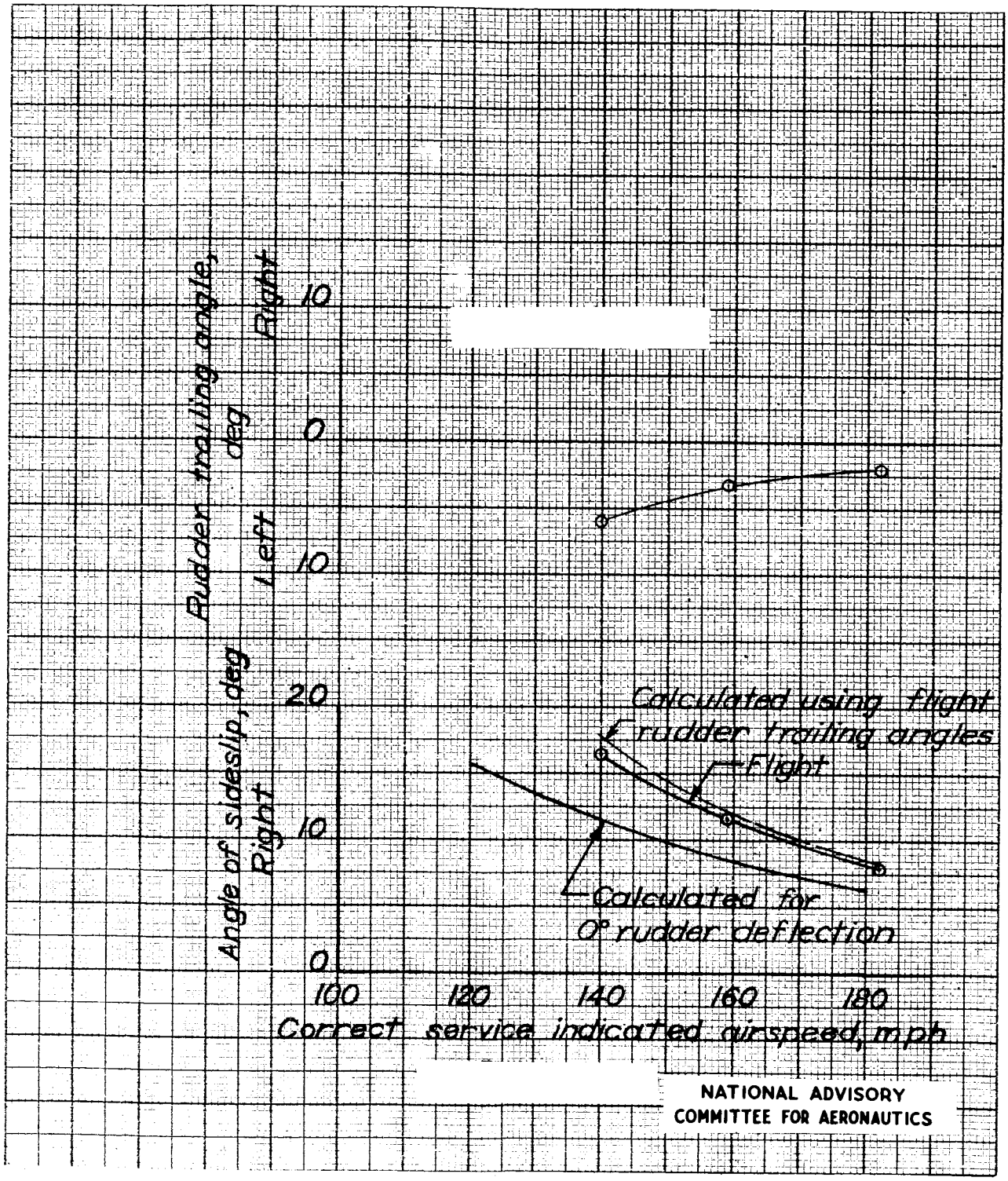

Figure 17. - Variation with the rudder fixed and with the rudder free of the sideslip angle for trim with airspeed, left engine idling, right engine delivering rated power, flaps up, Douglas A-26B airplane.

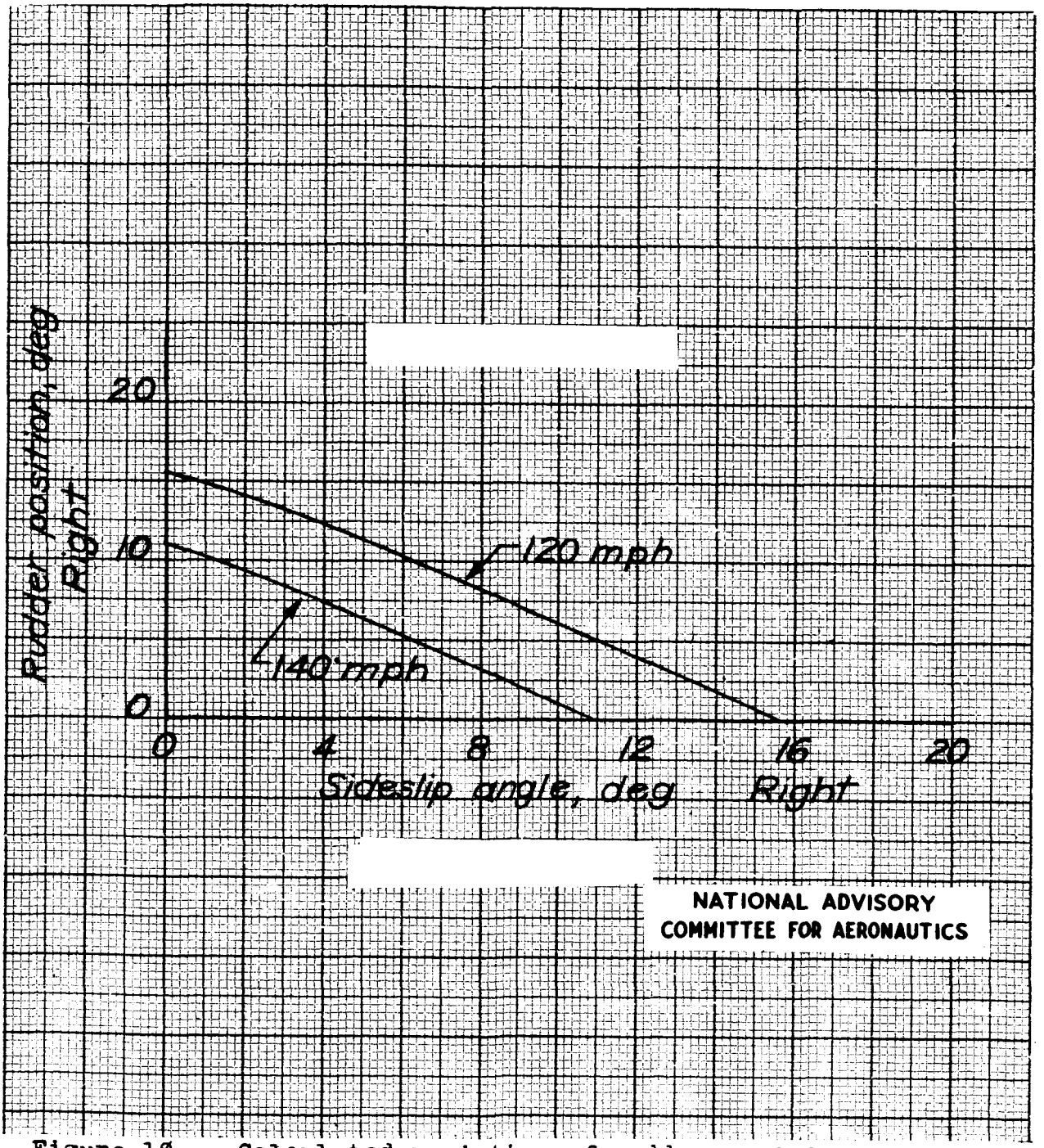

Figure 18. - Calculated variation of rudder position with sideslip angle at 120 and 140 miles per hour with left engine idling, right engines at normal rated power, flaps up, Douglas A-26B airplane.